INTERFACE

rsif.royalsocietypublishing.org

Research

Cite this article: Zhao S, Brady PC, Gao M, Etheredge RI, Kattawar GW, Cummings ME. 2015 Broadband and polarization reflectors in the lookdown, *Selene vomer*. *J. R. Soc. Interface* **12**: 20141390.
http://dx.doi.org/10.1098/rsif.2014.1390

Received: 20 December 2014
Accepted: 20 January 2015

Subject Areas:
biophysics

Keywords:
iridophores, guanine platelets, the lookdown, broadband reflectance, polarization, camouflage

Author for correspondence:
Shulei Zhao
e-mail: szhao@utexas.edu

Electronic supplementary material is available at http://dx.doi.org/10.1098/rsif.2014.1390 or via http://rsif.royalsocietypublishing.org.

THE ROYAL SOCIETY PUBLISHING

Broadband and polarization reflectors in the lookdown, *Selene vomer*

Shulei Zhao[1], Parrish Clawson Brady[1], Meng Gao[2], Robert Ian Etheredge[1], George W. Kattawar[2] and Molly E. Cummings[1]

[1]Department of Integrative Biology, University of Texas, Austin, TX 78712, USA
[2]Department of Physics and Astronomy, Texas A&M University, College Station, TX 77843, USA

Predator evasion in the open ocean is difficult because there are no objects to hide behind. The silvery surface of fish plays an important role in open water camouflage. Various models have been proposed to account for the broadband reflectance by the fish skin that involve one-dimensional variations in the arrangement of guanine crystal reflectors, yet the three-dimensional organization of these guanine platelets have not been well characterized. Here, we report the three-dimensional organization and the optical properties of integumentary guanine platelets in a silvery marine fish, the lookdown (*Selene vomer*). Our structural analysis and computational modelling show that stacks of guanine platelets with random yaw angles in the fish skin produce broadband reflectance via colour mixing. Optical axes of the guanine platelets and the collagen layer are aligned closely and provide bulk birefringence properties that influence the polarization reflectance by the skin. These data demonstrate how the lookdown preserves or alters polarization states at different incident polarization angles. These optical properties resulted from the organization of these guanine platelets and the collagen layer may have implications for open ocean camouflage in varying light fields.

1. Introduction

Fish use the coloration and reflectance of their skins for camouflage. To reduce visibility, a fish must match the spectral, intensity and perhaps polarization components of the environment [1–4]. The open ocean presents an additional challenge for camouflage as the light field can vary dramatically throughout the day. When the optical environment in the open ocean is largely homogeneous (e.g. cloudy days or in deeper waters), a specular broadband reflector is expected to serve crypsis very well [1,5]. However, when the light field is asymmetric (e.g. near the ocean surface on sunny days) in terms of intensity [6] and polarization [4], crypsis is expected to involve reflectance properties dependent on the angle of observation or possible behavioural modifications [2,4]. Here, we explore how a silvery open ocean fish, the lookdown (*Selene vomer*), achieves both broadband reflectance and unique polarization reflectance properties via its integumentary components.

Light fields in the open ocean are produced by direct sunlight and scattering and absorption properties of the water column. Under cloudy skies or in the deeper water column, the radiance field surrounding the fish is largely symmetrical around an axis perpendicular to the water surface [7,8]. Given this axial symmetry, Denton and colleagues suggested that organisms that reflect light similar to a specular broadband mirror held vertically would match their background from any angle of observation [1,9]. The silvery surfaces of many species of fish are considered to be good broadband reflectors [10]. Reflection by these fish is primarily caused by stacks of the guanine crystal platelets in iridophore cells in the skin. Denton and colleagues proposed the first model to explain the high reflectivity in fish skin in which stacks of guanine platelets are considered as ideal multilayer reflectors, each layer with an optical thickness of a quarter of the wavelength of light that the stack is intended to reflect [10]. This model provides a good explanation for the narrow-band coloured iridescence in some

fish [11,12], but it is unsatisfactory in explaining the broadband reflectance by silvery fish.

Since the 1970s, several different models have been proposed to explain broadband reflectance in biological organisms. These models all attribute broadband reflectance to variation in the reflecting elements along the dimension perpendicular to the reflecting surface. Parker *et al.* [13] reviewed three configurations that can produce broadband reflectance: multi-stacked, chirped and chaotic. A multi-stack configuration consists of several different types of multilayer stacks. Each type of stack has a spacing between reflecting platelets different from other types and is tuned to a specific wavelength [10]. In the chirped configuration, the spacing between the reflecting platelets changes progressively throughout the depth of the structure [10,14]. In a chaotic configuration, the thickness of reflecting elements and the spacing between them are random [15]. The chirped stack model has been found in beetles [13,16], and the other two models have been found in various fish species [15,17].

Here, we present an additional model for broadband reflectance as demonstrated in the lookdown. This model consists of densely packed stacks of small guanine platelets. These individual stacks contain platelets with a uniform spacing but their yaw orientations are random. Broadband reflectance is produced from increased scattering events combined with mixing of different colours resulted from these platelet stacks tilted at various angles. This type of configuration produces distinct colours on a micro-scale level, but these colours are spatially mixed to result in the perception of broadband reflectance. This type of colour mixing has been observed in other animal reflectance such as in some beetles [18] and butterflies [19].

In some ocean environments where the light field is largely unpolarized, broadband reflectors that are non-polarizing would be optimal concealers [20]. However, it is becoming increasingly apparent that light fields in many marine environments are highly polarized and can be quite heterogeneous [21–23]. Researchers have noted for years that the near-surface light field, dominated by direct sunlight, is not axially symmetric in intensity and polarization particularly when the sun is low on the horizon [1,2,4,6,21,23]. In these conditions, both the angle and degree of polarization vary around the fish. Our recent work shows that the polarization states of the light reflected by the lookdown were preserved when the incident polarization plane was aligned with the anterior–posterior or dorsal–ventral axis of the fish, but they were altered when the polarization plane deviated from these axes [4]. These reflectance properties reduced the overall polarization contrast with its background under the asymmetric polarized radiance fields associated with low solar inclinations in the ocean [4]. This finding suggests a potential strategy for camouflage by marine fish in the open ocean environment and prompted us to investigate the organization and optical properties of the reflecting elements in the skin of the lookdown.

In this study, we analyse the morphology and three-dimensional organization of the guanine platelets in the skin of the lookdown using light microscopy and scanning electron microscopy (SEM) to understand how light is reflected from the surface of the fish. We also analyse the optical properties of these guanine platelets such as birefringence and partial angular distribution of reflectance. We present an additional model for broadband reflectance and support it with computational simulation. Our data suggest that the angle-dependent alteration of polarization states by the lookdown observed by Brady *et al.* [4] appear to be a combined effect of birefringence properties of the guanine platelets/the collagen layer in the skin and the random phase changes as light is reflected from multiple layers of guanine platelets. These results may help to better understand animal reflectance and camouflage in the aquatic environment.

2. Material and methods

2.1. Skin preparations and pitch angle measurements

Fish skins (approx. 1 cm^2) with the underlying muscle were cut with a sharp razor from the flanks of the lookdown ((figure 1*a*) as described in the electronic supplementary material. For imaging analysis, the surface of the skin was covered with a 50% glycerol prepared in phosphate-buffered saline (PBS) followed by cover glass. Images of the surface of the skin were taken with a Leica stereomicroscope (Leica M205 C) at a low resolution (0.78× objective) and at a higher resolution (16× objective). To analyse the guanine platelets in the skin, scales and the collagen layer (stratum compactum) above the iridophores (figure 1*d*) were carefully removed with fine forceps under a dissecting microscope. The skin preparation was placed on a microscope slide with the muscle side facing down and covered with 50% glycerol in PBS followed by cover glass for imaging by a Nikon Eclipse 80i microscope with epi-illumination. Pitch angles of the long axes of guanine platelets with respect to the dorsal–ventral axis of the fish (figure 3*c–e*) were measured using NIH's ImageJ software.

2.2. Scanning electron microscopy analysis

The fish skin was removed as described above and fixed in 2% glutaraldehyde and 2% formaldehyde in PBS overnight at 4°C. The tissue was rinsed with distilled water before cross and horizontal sections (1.5–2 mm in thickness) were cut with sharp razors. Definitions of these sections are illustrated in figure 1*b*. These tissue sections were again rinsed with distilled water and dehydrated for 15 min in each of the increasing concentrations of ethanol (50, 75, 95 and 100%) followed by drying in a critical-point drying instrument (Tousimis Samdri-790). Dried specimens were coated with palladium/platinum using Cressington 208 Sputter Coater and analysed by SEM (Zeiss Supra 40 VP). Images of horizontal sections were used to measure the yaw angles of guanine platelets' short axes with respect to the skin's surface (β in figure 4*c*) using ImageJ software.

To expose the reflecting surfaces of the guanine platelets, skin tissues embedded in the freezing medium were sectioned on a cryostat parasagittally (parallel to the surface of the skin; see figure 1*b*) and mounted on microscope slides and rinsed with distilled water and dehydrated with increasing concentrations of ethanol as described above. The specimens were air-dried for at least 2 h. The microscope slides with the tissue sections were cut into smaller pieces and attached to SEM mounts for coating and SEM imaging.

2.3. Modelling the reflectance of the iridophore layer

To better understand the reflectance property of guanine platelets in the lookdown, we simulated light propagation and reflection in the densely packed guanine platelet layer. To consider multiple scattering events directly, we modelled this iridophore layer as a collection of platelet stacks (see figures 4*b* and 5*b*). For simplicity, each stack contains four platelets with a width of 1 µm (see electronic supplementary material, table S3) that account for the finite-size effect on their scattering properties [24,25]. As the iridophore layer has translational symmetry along the long axis of the platelets, we approximated the iridophore layer as a two-dimensional system. The reflectance spectrum of the modelled iridophore system was simulated with the

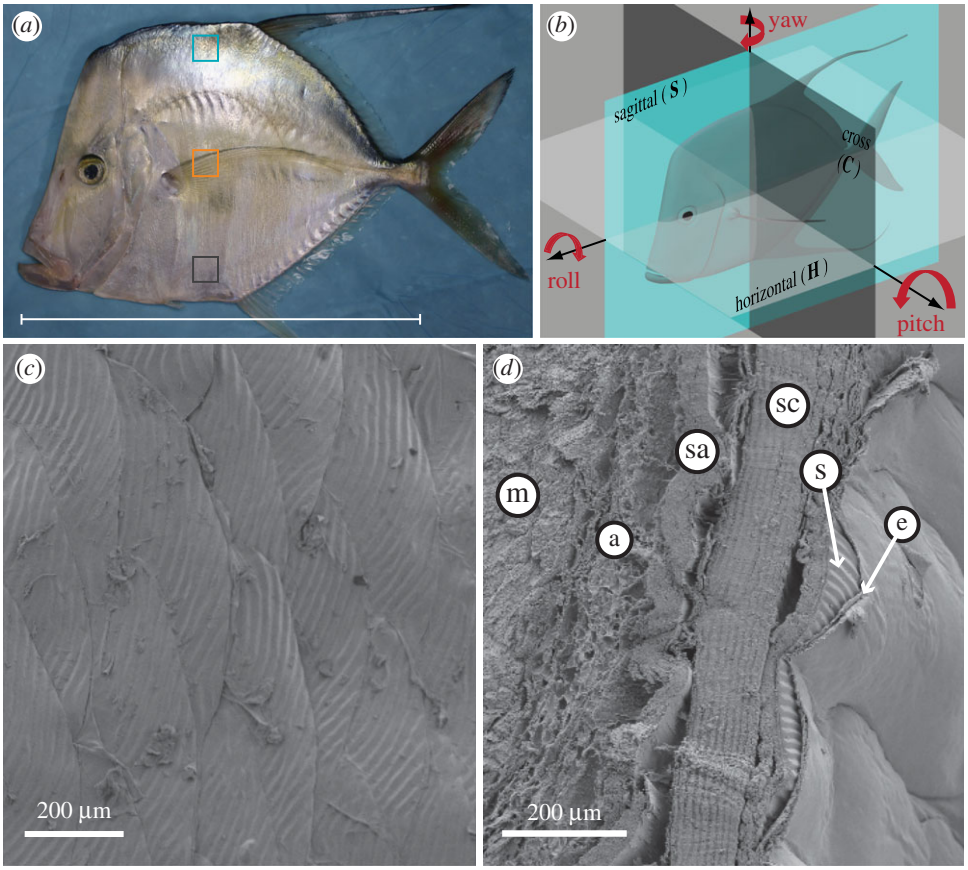

Figure 1. (*a*) The lookdown, *Selene vomer*. The blue, orange and grey squares are the regions of interest in the dorsolateral, mid-lateral and ventrolateral flanks described in the text, respectively. The average standard length of the fish (white bar) used in this study was 19.6 ± 1.3 cm (mean ± s.d., $n = 5$). (*b*) Illustration of cross (C), horizontal (H) and sagittal (S) sections used for histological analysis. A cross (or transverse) section is perpendicular to the anterior–posterior axis of the fish. A horizontal section is parallel to the anterior–posterior axis of the fish and divides the fish into dorsal and ventral parts. A sagittal section contains the fish's anterior–posterior axis and divides the fish into left and right halves. A parasagittal section is parallel but lateral to the sagittal section. Because the lookdown has a very flat body, we call sections parallel to the fish surface as parasagittal in this study. Roll, pitch and yaw angles of guanine platelets with respect to the fish surface were examined to determine their three-dimensional orientation. (*c*) A SEM image of the ventrolateral surface of the lookdown shows an array of overlapping oval-shaped scales with average short and long axes being 460 ± 65 µm and 744 ± 101 µm (mean ± s.d., $n = 71$), respectively. (*d*) A SEM image of a horizontal section of the skin from the mid-flank region shows the epidermis (e), the scales (s), the collagen layer, also known as stratum compactum (sc) of dermis, the stratum argenteum (sa) consisted of iridophores containing guanine platelets, a patch of adipose cells (a) and the muscle (m). The curvature of the iridophore layer was an artefact resulted from tissue drying.

finite-difference time-domain (FDTD) method [26]. The FDTD method calculates the scattering electric and magnetic fields by solving the Maxwell equations through discretizing both the time and spatial domains. The reflectance was obtained from the ratio of the reflected and incident power across specific detectors (figure 6*a*). The MEEP package was used to conduct the FDTD simulation in a two-dimensional system [27].

Measured dimensions from SEM and light microscopy were used in the modelling (the guanine platelet thickness = 0.1 µm; the spacing between consecutive platelets = 0.2 µm). The stacks were randomly positioned in the system (figure 6*a*). The density of the platelets used in the simulation was approximately 2 platelets μm^{-2}, slightly lower than the measured value. Orientations of the platelets followed Gaussian distribution (figure 4*c*). The depth of the system was 70 µm as measured for the Type 4 platelet layer (electronic supplementary material, figure S1). The width of the system was chosen as 20 µm, much greater than that of a single platelet. The refractive indices for the guanine platelet and the intracellular medium were 1.83 and 1.33 [20], respectively. Birefringence of the guanine material was neglected. A periodic boundary condition was imposed on the left and right boundaries of the system in order to approximate a system with infinite horizontal dimension. A plane wave from a light source with a wavelength from 0.4 µm to 0.8 µm and a spatial resolution of 0.01 µm was used for the simulation. All reported wavelengths are defined in air. The reflectance of an unpolarized incident light field was calculated by averaging the simulated reflectance of an incident plane wave with polarization perpendicular and parallel to the two-dimensional system. For comparison, the reflectance spectrum from the ventral flank of the lookdown was measured using a spectrometer with a fibre-optic probe as described in the electronic supplementary material.

2.4. Birefringence of the surface and skin sections

Birefringence of the surface and skin sections of the lookdown were evaluated by cross-polarization microscopy. Cross-polarization images were collected as the fish was rotated from its natural swimming position by 22.5°, 45°, 67.5° and 90°. Sections of the lookdown's skin and the collagen layer were also analysed similarly. The detailed procedures are described in the electronic supplementary material.

3. Results

3.1. The anatomy of the lookdown's skin

The lookdown's body is rhombus-shaped and laterally compressed. It appears silvery on lateral flanks with darker and

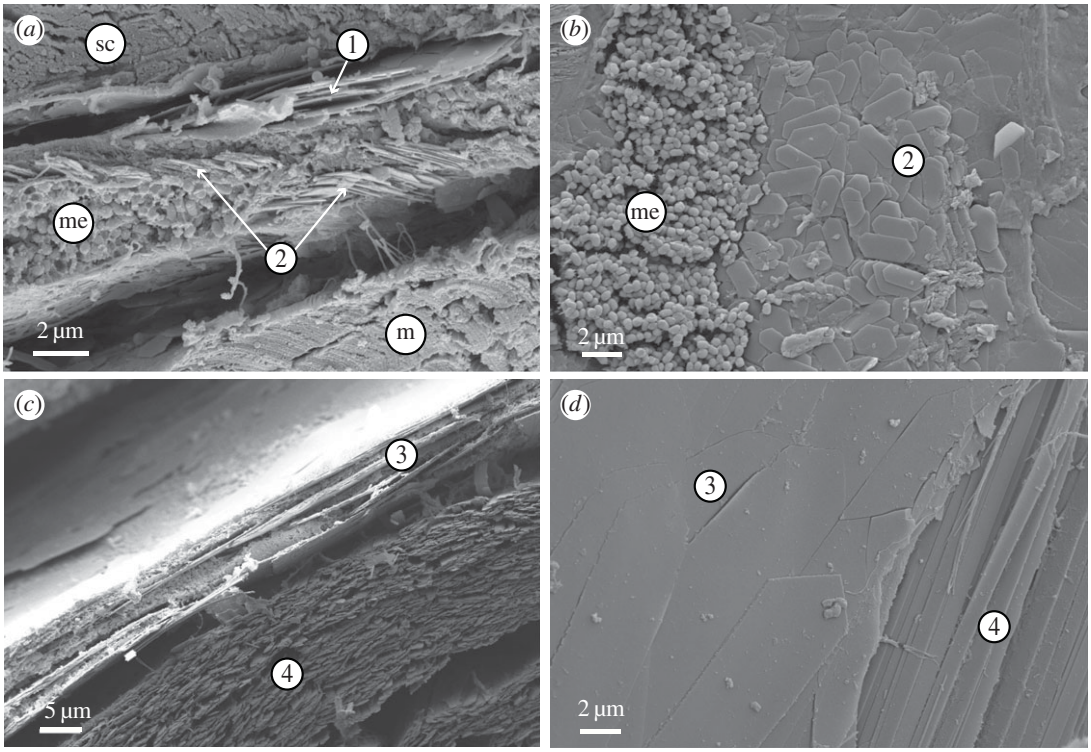

Figure 2. SEM images of the lookdown's skin sections from the dorsolateral (*a*,*b*) and mid-lateral (*c*,*d*) flanks. (*a*) A cross section shows Type 1 and Type 2 guanine platelets (arrows), melanosomes (me), stratum compactum (sc) and muscle (m) in the dorsolateral flank. (*b*) A parasagittal section of the dorsolateral skin shows melanosomes and Type 2 guanine platelets with various pitch orientations. (*c*) A horizontal section of the mid-lateral flank shows Type 3 and Type 4 guanine platelets. (*d*) A parasagittal section of the mid-lateral skin shows Type 3 and Type 4 guanine platelets.

blue tints above the lateral line (figure 1*a*). The yellow tone of the lookdown's surface results from the presence of xanthophores in the skin. The scales of the lookdown are very small, thin and transparent, and cannot be identified by naked human eyes (figure 1*c*).

To analyse the three-dimensional organization of the guanine platelets in the lookdown's skin, we define the line connecting the eye and the centre of its caudal peduncle as the anterior–posterior axis of the lookdown (figure 1*b*). This line remains essentially parallel to the surface of the water as the lookdown swims naturally. The skin tissues of the lookdown were sectioned at three different planes: cross (C), horizontal (H) and sagittal (S) (or parasagittal) as shown in figure 1*b*. The SEM image of a horizontal section showed that the stratum compactum (sc) and stratum argenteum (sa) contributed to the bulk part of the lookdown's skin (figure 1*d*). The stratum compactum consisted primarily of collagen layers, while the stratum argenteum consisted primarily of iridophores. The scales (s) lay on top of the stratum compactum and were covered by a thin epithelial layer (e). Adipose tissue (a) was often seen between the stratum argenteum and the muscle (m). The 'yaw' angles of the guanine platelets were examined in horizontal sections.

A cross section (figure 1*b*) is perpendicular to the anterior–posterior axis and used to examine the 'roll' angle of the guanine platelets. In the cross section, the long axes of the guanine platelets were parallel to the surface of the fish (see electronic supplementary material, figure S1). A sagittal section contains the anterior–posterior axis and divides the fish into left and right parts. A parasagittal section is lateral to the sagittal section but remains parallel to it. It was used to examine the 'pitch' angle and morphology of the guanine platelets (figure 1*b*).

3.2. Four types of guanine platelets

SEM analysis of the skin sections revealed the presence of four types of guanine platelets in the stratum argenteum of the lookdown's skin. Two types were present in the dorsolateral argenteum, named Type 1 and Type 2 (figure 2*a*,*b*). Type 1 guanine platelets were closer to the surface of the skin and next to the stratum compactum. Underneath the Type 1 guanine platelets were the much smaller Type 2 guanine platelets. The melanophores in the region were surrounded by iridophores containing Type 2 guanine platelets (figure 2*a*,*b*). All Type 1 platelets appeared to be parallel to the surface of the skin, while Type 2 guanine platelets exhibited various orientations.

In the mid-lateral and ventrolateral flanks of the lookdown, there were two additional types of guanine platelets, Type 3 and Type 4 (figure 2*c*,*d*). These two types of guanine platelets can be readily distinguished by their widths with Type 3 being much wider than Type 4. The long axes of these two types of guanine platelets exhibited similar pitch angles (figure 2*d*). The Type 4 guanine platelets formed a thick layer (electronic supplementary material, figure S1*e*,*f*) and were densely packed (figure 2*c*). The morphologies and dimensions of these four types of guanine platelets are better illustrated in SEM images of dissociated guanine platelets (electronic supplementary material, figure S2).

3.3. Broadband reflectance of the lookdown's skin

The ventrolateral skin of the lookdown is silvery. When placed under a dissecting microscope at low magnification, the skin still appeared silvery (figure 3*a*). However, at higher magnification, the image of the skin became a multi-coloured mosaic with orange, yellow, green and blue/purple colours (figure 3*b*).

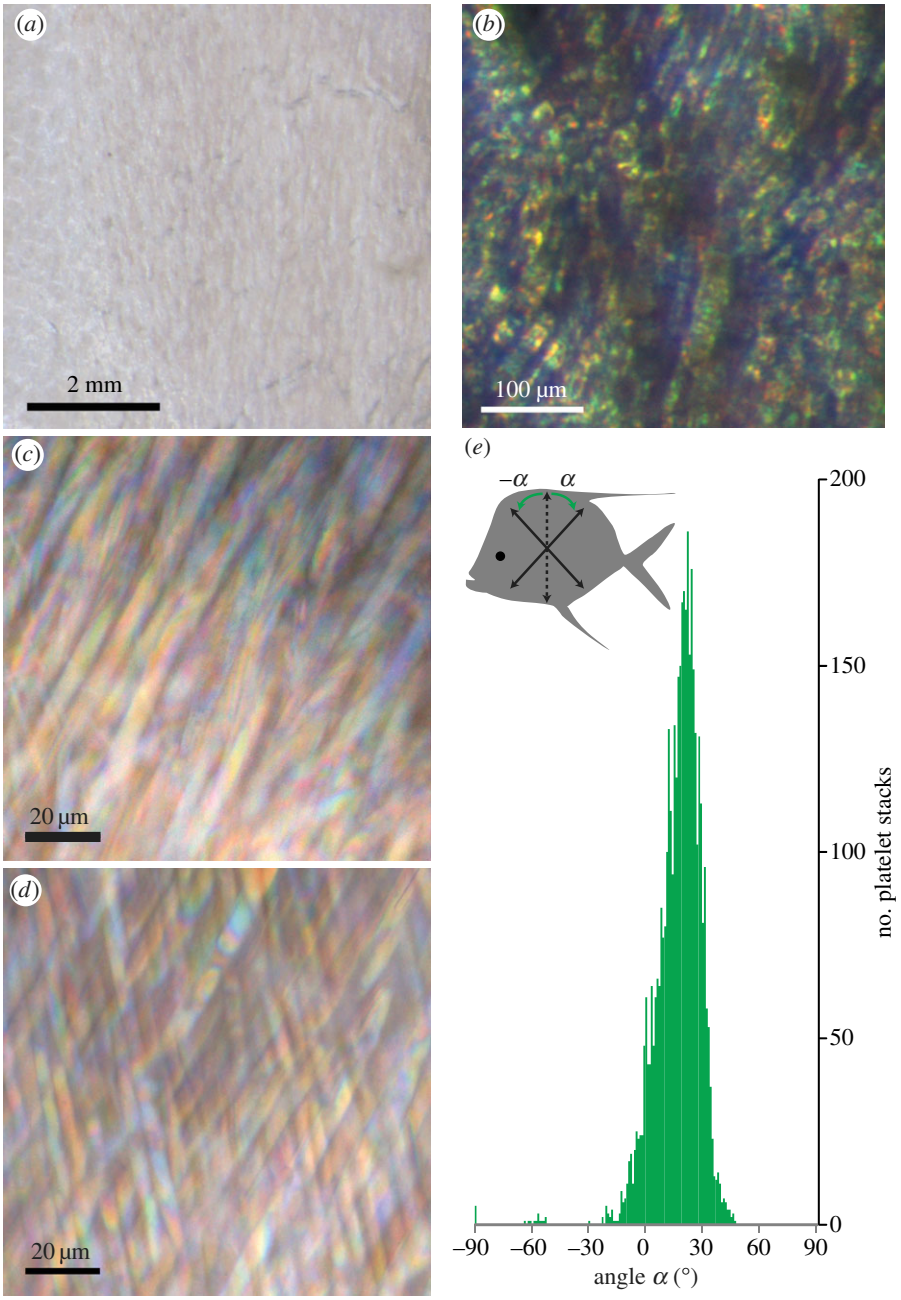

Figure 3. Silvery skin and pitch angles of guanine platelets. (*a*) A low-magnification image shows the silvery skin from the ventrolateral flank. (*b*) A higher magnification image of the same region as in (*a*) shows multiple colour patches. (*c*) Removal of the scales and the collagen layer revealed stacks of multi-coloured Type 3 guanine platelets in the mid-lateral flank with epi-illumination. The guanine platelets were oriented predominantly in one direction. (*d*) In some areas of the mid-lateral skin, two distinct orientations of Type 3 platelets were observed. (*e*) Histogram of the pitch angles of the guanine platelets. With the fish orientation as illustrated in the pictograph, the pitch angle of a platelet (α) is defined as positive or negative if it is tilted away from the vertical line clockwise or counter-clockwise, respectively. The orientation of fish skin samples in (*a*–*d*) is the same as the fish pictograph in (*e*). Pitch angles of the guanine platelets in the mid-lateral flank showed an average of 17.3° ± 11.0° (mean ± s.d.) and the peak between 22° and 23°.

This demonstrated that our perception of broadband reflectance resulted from spatial mixing of multiple colours in small areas that were indistinguishable to naked human eyes. This broadband reflectance was confirmed by measured reflectance spectrum from the lookdown's skin (figure 6*c*).

3.4. The pitch angle of the platelets

After removal of the scales and the collagen layer from the mid-lateral or ventrolateral skin, Type 3 guanine platelets were readily seen under light microscopy with epi-illumination. The majority of the guanine platelets exhibited a pitch orientation as shown in figure 3*c*. Using the definition for the positive (α) and negative ($-\alpha$) pitch angles illustrated in figure 3*e*, quantitative analysis of these angles showed that the majority of platelets had positive pitch angles with the highest frequency occurring between 22° and 23°. Also often observed were two sets of iridophores with distinct platelet orientations, one with positive pitch angles and the other with negative pitch angles (figure 3*d*). This pattern of guanine platelets accounted for nearly all the platelets with negative pitch angles shown in the histogram (figure 3*e*). The statistical mean of the pitch angles of Type 3 guanine platelets in the mid-lateral flank was 17.3° ± 11.0° (mean ± s.d.; $n = 4041$).

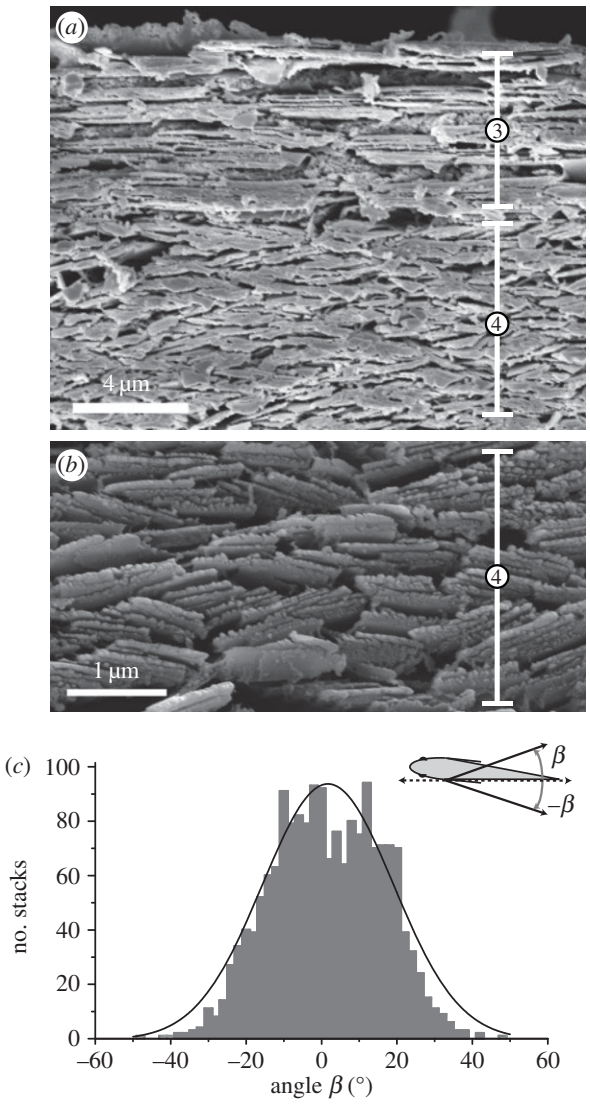

Figure 4. Yaw angles of the guanine platelets. (*a*) SEM image of a horizontal section from the mid-lateral flank shows that the short axes of the Type 3 platelets are parallel to the surface of the skin (horizontal), while those of Type 4 platelets exhibit various orientations. (*b*) A higher magnification SEM image shows Type 4 platelets with various yaw angles. (*c*) Histogram of yaw angles of Type 4 platelet stacks exhibited Gaussian distribution. Definitions of positive (β) and negative ($-\beta$) yaw angles between the surface of the fish and the short axes of the platelets are shown. The average yaw angle was $0.59^\circ \pm 14.59^\circ$ (mean $\pm$ s.d., $n = 1761$).

It should be pointed out that Type 4 guanine platelets underlay Type 3 platelets and were not visible in figure 3*c*,*d*. The pitch angles of the Type 4 guanine platelets appeared to be similar to those of Type 3 (figures 2*d* and 7*b*1–*b*6).

3.5. The roll and yaw angles of the platelets

The roll angles of the long axes of both Type 3 and Type 4 guanine crystals were parallel to the surface of the skin (electronic supplementary material, figure S1*b*,*c*,*e*,*f*). The short axes of Type 3 platelets was also parallel to the surface of the skin (yaw angle = 0°; figure 4*a*). However, the short axes of Type 4 platelets exhibited random yaw angles (figure 4*b*). Quantitative analysis of their orientations showed that the distribution of the yaw angles with respect to the surface of the skin resembled Gaussian distribution (χ^2 test: $\chi^2 = 75.62$; d.f. = 99, $p > 0.95$) (figure 4*c*). The average yaw angle was $0.59^\circ \pm 14.59^\circ$ (mean $\pm$ s.d., $n = 1761$). This random yaw orientation of guanine platelets has significant implications for reflection of light coming from different directions.

3.6. The organization of the guanine platelets

Based on information obtained from light microscopy and SEM, the organizations of guanine platelets in the dorsolateral and ventrolateral regions of the lookdown's skin are illustrated in figure 5*a*,*b*. These illustrations represent horizontal sections. Types 1 and 2 guanine platelets in the dorsolateral flank have a much smaller length to width ratio than Types 3 and 4 in the mid-lateral and ventrolateral flanks. In the dorsolateral skin, Type 1 platelets form a thicker layer than Type 2 (electronic supplementary material, figure S1*d*). The melanophores in this region are surrounded by iridophores containing Type 2 platelets. In the mid-lateral or ventrolateral flanks, the vast majority of the guanine platelets in the regions are of Type 4 that forms a much thicker layer than Type 3 (electronic supplementary material, figure S1e,*f*).

In the lookdown's skin, reflecting guanine platelets were found present only in the stratum argenteum in the dermis. No guanine platelets were observed in the epidermis or associated with the scales. The total thickness of the iridophore layer increased progressively from the dorsolateral region to the ventrolateral region primarily due to increase in the number of Type 4 platelets (electronic supplementary material, figure S1*h*). This is believed to contribute to the increased broadband silvery reflectance in the mid-lateral and ventrolateral flanks.

Among the four types of guanine platelets, Type 1 and Type 3 have relatively large surface areas and are closer to and parallel to the surface of the skin. Type 2 and Type 4 guanine platelets have smaller surface areas and are always underneath Type 1 and Type 3 platelets, respectively. Both the long and short axes of Type 2 platelets exhibited various orientations. The long axes of Type 4 guanine platelets are parallel to the fish surface but their short axes exhibit random yaw angles with respect to the surface of the skin (figure 4*b*). The first layer of iridophores containing large guanine platelets (Type 1 and Type 3) appears to function as regular multilayer reflectors. The second layer consisting of smaller guanine platelets (Type 2 and Type 4) with various orientations may function as broadband semi-diffusers. In the dorsolateral skin, Type 1 (the regular reflector) is the predominant guanine platelet producing primarily an iridescent blue colour (figure 1*a*). In the mid-lateral or ventrolateral skin, Type 4 is the predominant guanine platelet thus producing a broadband silvery shine. Low-intensity iridescence can also be observed in the mid-lateral to ventrolateral flanks. The colour of the iridescence in these regions varies from orange to green, blue or purple depending on the angle of observation.

3.7. Modelling reflectance of the Type 4 iridophore layer

To determine the spatial variations in reflectance, two detectors with width of 20 µm (*d*1) and 2 µm (*d*2), respectively, were used for the reflectance simulation (figure 6*a*). Only the reflected light passing through the detector was accounted for in the calculation. The simulated spectra were averaged from reflectance

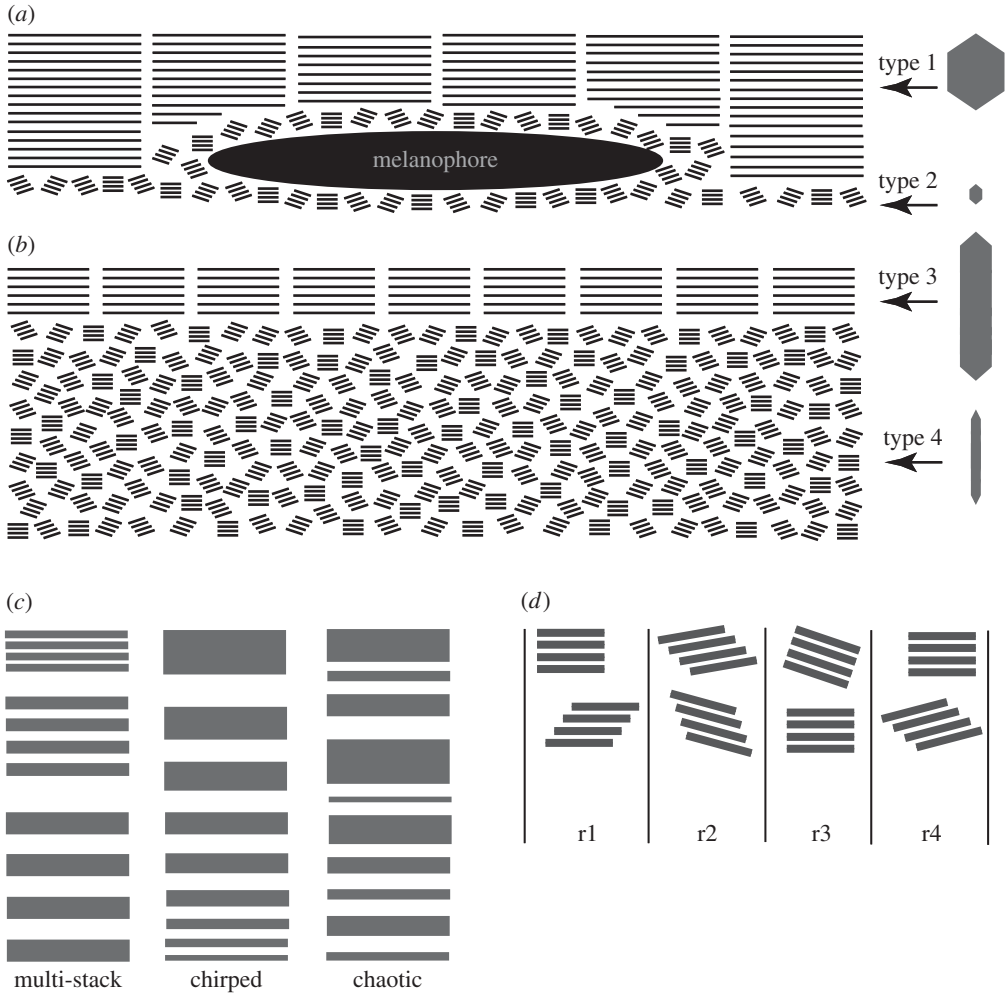

Figure 5. The organization of the guanine platelets in the horizontal section of the lookdown's skin and models for broadband reflectance. (*a*) The arrangement of Type 1 and Type 2 guanine platelets and melanophores (me) in the dorsolateral skin. Long and short bars represent Type 1 and Type 2 guanine platelets, respectively. (*b*) The arrangement of Type 3 and Type 4 guanine platelets in the mid-lateral or ventrolateral skin. Long and short bars represent Type 3 and Type 4 guanine platelets, respectively. The morphologies of these guanine platelets are illustrated at the right side of the figure. (*c*) Three existing radial variation models for broadband reflectance by silvery fish: the multi-stack, chirped and chaotic models. (*d*) The lateral variation model for broadband reflectance. For simplicity, only two stacks of guanine platelets in four of many possible arrangements are illustrated (r1–r4). Variations in spacing and orientation among platelet stacks exist in these four different regions.

of 10 randomly generated configurations. Different configurations resulted in slightly different reflectance spectra as indicated by the error bars in figure 6*b*. The reflectance detected by detector *d*1 accounted for all the reflected light in the system and had a relatively flat spectrum with small variations. By contrast, detector *d*2 received light in a much smaller window. The average reflectance detected by *d*2 was similar to that by *d*1, but with much larger variations. This supports our experimental observation that colour varied among small areas (detected by *d*2) and the perceived broadband reflectance (detected by *d*1) resulted from colour mixing. The calculated spectra could be further flattened by including more complexity observed in the real tissue, such as the sheer and variation in the number of platelets in stacks (figure 4*b*). For comparison, the calculated reflectance spectrum of a four-platelet layer is shown as the solid black line (figure 6*b*). These four platelets had the same spacing as in the platelet stacks shown in figure 6*a* but with an infinite radius and were all parallel to the surface. The actual reflectance spectrum measured from the ventrolateral flank of the lookdown is shown in figure 6*c*. As the reflectance of this type of platelet organization shown in figure 6*a* can be enhanced by constructive interference, this effect may enable the iridophore system to be more efficient in reflecting light than other diffuse reflecting biological structures, such as leucophores [28].

3.8. Birefringence of the lookdown's skin

To evaluate the effect of the lookdown's surface on polarized light, juvenile lookdowns were analysed under the dissecting microscope with crossed polarization filters. The optical axis of the sample was established by rotating the fish and determining the orientation where the minimum and maximum intensities of the image were detected, which should be 45° apart. The optical axis should be aligned with or perpendicular to the orientation with the lowest intensity. The mid-lateral flank image of the lookdown exhibited minimum intensity when the polarization of the incident light was aligned with its anterior–posterior or dorsal–ventral axis (figure 7*a*2, *a*6). Maximum intensity was observed when the anterior–posterior axis of the fish had an angle of about 45° with respect to the polarization plane of the incident light (figure 7*a*4). The observed birefringence effect cannot

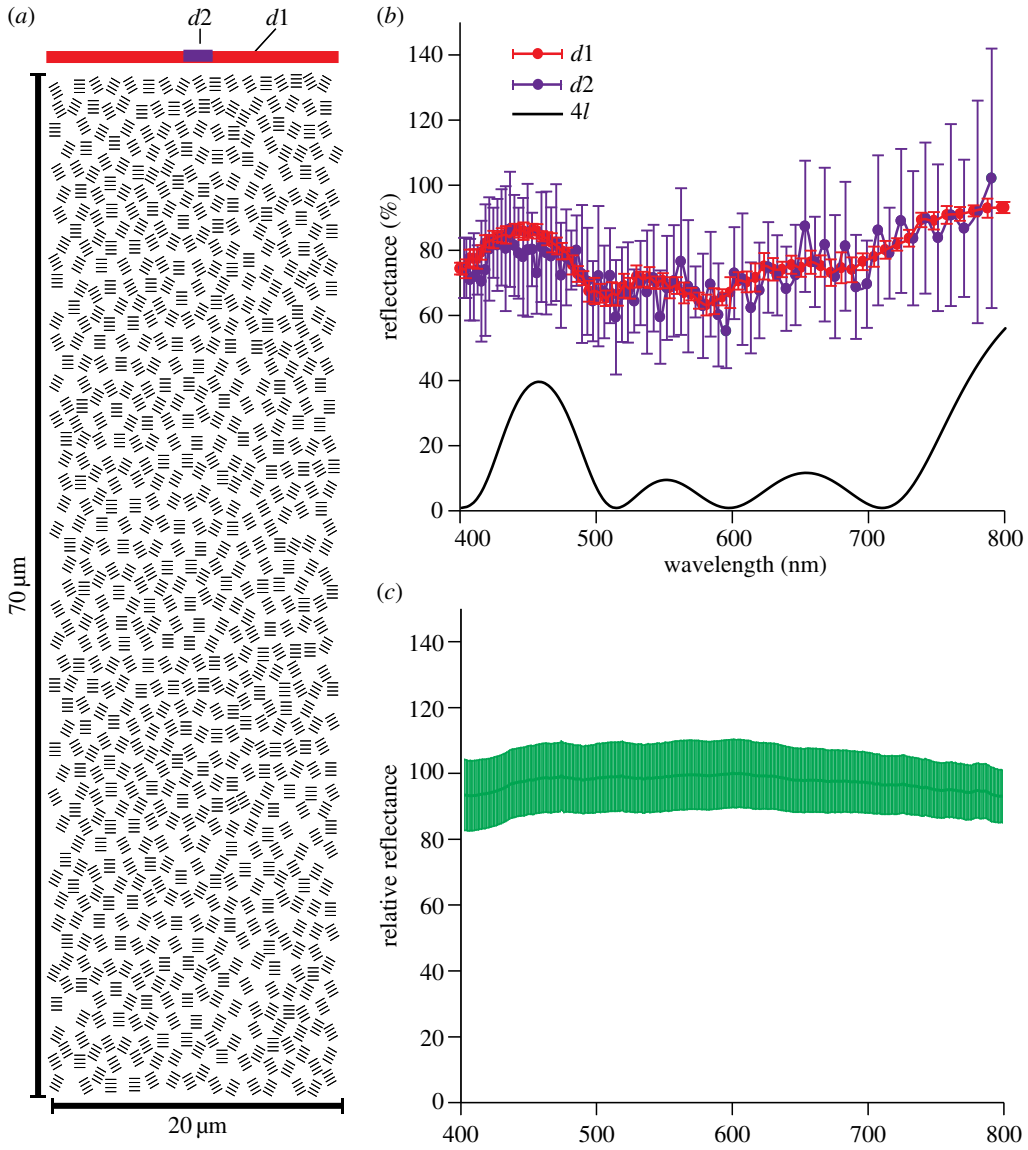

Figure 6. Reflectance from simulation and measurement. (*a*) The configuration of guanine platelet stacks for simulation. Each stack consists of four individual platelets. The orientation of the stacks follows the Gaussian distribution. The widths of detectors *d*1 and *d*2 are 20 µm and 2 µm, respectively. (*b*) Average reflectance from simulations of 10 randomly generated configurations. Error bars represent standard deviations. Reflectance detected by *d*1 is a relatively flat spectrum with small variations. Average reflectance detected by *d*2 is similar to that by *d*1, but with much greater variations. This suggests that colour variation between small areas is highly likely. The black solid line shows the reflectance spectrum (by *d*1) of four layer platelets with the same dimension as the platelet stack in (*a*) but all parallel with the surface and with an infinite radius. (*c*) Reflectance measured from the ventrolateral flank of the lookdown. The dark green line in the middle is the average spectrum of nine measurements. The light green shade marks the standard deviations of the measurements.

be due to dichroism which would result in the maximum intensity when the fish was rotated by 90° instead of 45°.

Birefringence of the guanine platelet layers from the mid-lateral flank was examined as the tissue section was rotated by a 22.5° increment from its original position. In the parasagittal sections (figure 7*b1–b6*), the optical axes of the guanine platelets were along long or short axes of the crystals. These platelets exhibited maximum effect of birefringence when their long or short axes were 45° with respect to the polarization plane of the incident light (figure 7*b4*).

The collagen layer covering the guanine platelets in the lookdown was also birefringent. Alteration of the polarization state was minimal (low intentsity) when the collagen layer maintained its natural orientation as on the fish (the anterior–posterior axis of the fish being horizontal) or when it was rotated by 90° (figure 7*c2*,*c6*). Maximum alteration of the polarization state occurred when the collagen sample was rotated by 45° from its natural orientation (figure 7*c4*). Quantitative analysis of intensity changes due to these birefringence effects is provided in the electronic supplementary material, figures S3 and S4.

4. Discussion

4.1. Broadband reflectance

Broadband reflectance by fish has been explained as a result of variation in the thickness of the reflecting platelets and/or in the spacing between these platelets. Denton & Land [10] suggested that broadband reflectance may result from multiple overlapping stacks of ideal multilayer reflectors (the multi-stack model) or a stack of reflectors with progressively

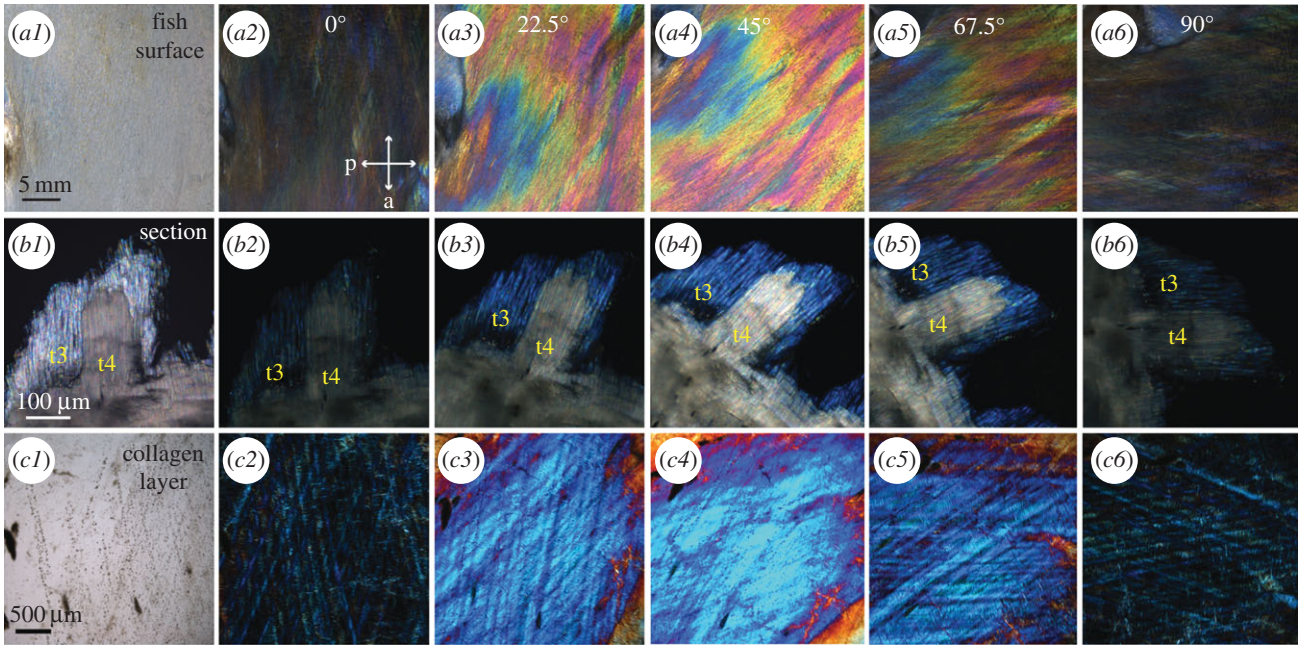

Figure 7. Birefringence of the intact surface of the lookdown's skin (*a2–a6*), the skin section (*b2–b6*) and the collagen layer (*c2–c6*) visualized by cross-polarization microscopy. (*a1*) An image of the mid-lateral flank of a juvenile lookdown was taken with unpolarized light. The anterior–posterior axis of the fish was horizontal with the fish's head on the left. (*a2–a6*) Cross-polarization images of the same view as in (*a1*) were taken as the fish was rotated from the horizontal position (0°) clockwise by 22.5°, and 45°, 67.5°, or 90°, respectively. The maximum intensity was observed at 45° (*a4*). The orientations of the polarizer (p) and analyser (a) are indicated by the arrows in (*a2*). (*b1*) An image of a parasagittal section of the mid-lateral skin was taken with unpolarized light as the long axes of the platelets were aligned with the analyser. (*b2–b6*) Cross-polarization images of the same view as in (*b1*) were taken as the tissue section was rotated from its original position (0°) clockwise by 22.5°, and 45°, 67.5°, or 90°, respectively. The long axes of Type 3 (t3) and Type 4 (t4) platelets were in the same orientation. They both had minimum visibility when their long axes were in vertical or horizontal position, while the maximum visibility was reached as the section was rotated by 45°. Type 3 platelets appeared blue, while Type 4 platelets were multi-coloured at high magnification and appeared nearly white at low magnification (*b4*). (*c1*) An unpolarized-light image of the collagen layer from the mid-flank with the same orientation as in the fish (*a1*). (*c2–c6*) Cross-polarization images of the collagen layer as it was rotated by 22.5°, and 45°, 67.5°, or 90°, respectively. The maximum intensity was observed at 45°.

changing optical thickness (the chirped model in figure 5*c*). McKenzie *et al*. [15] found that the thickness of guanine platelets and the spacing between them varied randomly in two fish species in the family Trichiuridae. A model based on this so-called chaotic structure (figure 5*c*) provides a good explanation for the broadband reflectance by the fish they studied. In all these three models, broadband reflectance results from variation of the reflector periodicity in the direction perpendicular to the surface of the fish. Therefore, we name them 'radial variation models' (figure 5*c*).

In our study, we found that perceived broadband reflectance from each of several species of silvery fish we examined consists of a mosaic of multiple colours at the microscopic level (e.g. figure 3*a*,*b*). These observations suggest that spatial colour mixing may be a universal mechanism for production of broadband reflectance in nature. The random orientation in the yaw angle of the Type 4 guanine platelets in the lookdown skin (figure 4) and the different ways that they are stacked together create variations not only in the direction perpendicular to the surface of the fish but also in all directions parallel to the surface. We name this type of broadband reflectance the 'lateral variation model' (figure 5*d*). This model does not exclude radial variation but takes into account variations both along the reflecting surface and in the direction perpendicular to it. We do not believe that any silvery fish relies strictly on radial variation to produce broadband reflectance.

A good example of this type of broadband reflectors is the wing of the butterfly *Argyrophorus argenteus* [19]. The silver colour of its wing results from the spatial mixing of multiple coloured thin strips produced by its scales. While random orientations of guanine platelets have been documented in other fish species (e.g. the Atlantic salmon [29] and the guppy [30]), this feature was not linked to broadband reflectance. McKenzie *et al*. [15] calculated reflectance from two fish species in the Trichiuridae family based on the chaotic model. They realized that their model deviated from the reality in two ways. One is that the spectral averaging obtained in their model was probably achieved in reality by spatial (or lateral) averaging in the skin. The other is that their model might have deviated from the actual structure in which the surfaces of guanine platelets might not always be parallel to the surface of the skin.

Incorporating the Gaussian distribution of Type 4 guanine platelets' yaw angles measured in the lookdown (figure 4*c*) into a model for computation, we found that these randomly positioned guanine platelets can function as a broadband reflector with increasing effectiveness as thickness of the layer increases (figure 6*a*,*b*). The dense packing of these platelets is essential in producing the broadband reflectance. As the multiple scattering is so strong, regardless of the direction and wavelength of the incident light, it always has a great probability of being reflected back. Variations in the thickness and orientation of individual platelets can help further flatten the spectrum but in a secondary manner. Variation in the platelets' yaw angles, however, can be important in producing diffuse reflectance by spreading the reflected light into a wider angular

range (electronic supplementary material, figure S6). As shown in figure 3*b*, multiple colours observed with high-magnification microscopy can be produced by varying the orientation of the platelets. Different orientations can change the interference path length, and thus vary the reflectance maxima for different wavelengths. Importantly, spectral reflectance measurements from the surface of the lookdown's skin confirm the model predictions that stacks of guanine platelets with random yaw angles in fish can serve as an effective broadband reflector. The same computational modelling method has recently been used to explain the diffuse whiteness in the pyjama squid [31].

4.2. Polarization reflectance

The unique arrangement of guanine platelets with random yaw angles (figures 4*b* and 5*b*), yet uniform in the roll (electronic supplementary material, figure S1) and pitch (figure 3) angles, is also expected to have a significant effect on polarization reflection. A previous study in our laboratory indicates that the specific polarization reflectance properties of lookdowns minimized polarization contrast throughout the day more effectively than the vertical mirror [4]. The ideal polaro-cryptic strategy for the near-surface open ocean environment involved reflectance properties that preserve reflected polarization along dorsal–ventral and anterior–posterior of the fish body and maximally depolarize the reflected light when the polarization is 45° from these axes. Our measurements of the intact surface of the skin and specific skin layers (guanine platelets and collagen) demonstrate that the lookdown's skin exhibits a high degree of birefringence (figure 7). Of interest is the finding that the optical axes of the guanine platelets and collagen layers are closely aligned, which result in the effective optical axis along one of the principal axes of the fish, thus conferring observed properties of polarization preservation or alteration.

4.3. Polarization preserving properties

The physical arrangement of the guanine platelets and the collagen in the lookdown's skin are consistent with the specific polaro-cryptic strategies required in an open ocean, near-surface environment [4]. The guanine platelet and collagen layers in the lookdown exhibit the highest degree of polarization preservation when the polarization of light is aligned with the fish's principal axes (0° and 90°; figure 7). Our analyses of the birefringence properties of the iridophore layer show consistency with those of individual guanine platelets observed in other marine fish [20]. These guanine platelets are weakly biaxial crystals [20] and their two optical axes are in two of the three possible directions: along the short or the long geometric axis (x or y axis within the reflecting surface), or perpendicular to the reflecting surface (z axis) (electronic supplementary material, figure S5). If one of the optical axes is along the z axis or the short geometric axis (x axis), these optical axes from individual platelet stacks with random yaw angles point to different directions but within a plane perpendicular to the long geometric axis of the crystals. When viewed normal to the fish skin, the projection of these optical axes to the x–y plane collectively produces an effective optical axis perpendicular to the long geometric axis of the crystals.

To investigate a birefringent reflector analytically, we estimate the phase differences accumulated in the reflection from the iridophore layer by examining the Type 4 guanine platelets. These platelets all have aligned pitch and roll angles but randomized yaw angles. Here, we assume that the phase difference, Γ, for light passing through the iridophore layer is

$$\Gamma(x, y) = \frac{2\pi(n_b - n_a)L(x, y)}{\lambda}, \tag{4.1}$$

where n_a and n_b are the refractive indices for the orthogonal polarization states that are 45° away from the incident e-vector; $L(x, y)$ is the length that the light wave passes through the iridophore layer before it is reflected, λ is the wavelength of light, and x and y are the coordinates on the surface of the skin [32]. When the polarization is aligned with the optical axes of this iridophore layer (parallel or perpendicular to the long axis of the guanine crystals), $n_b - n_a = 0$. Thus when the animal, in this case the lookdown, has a high degree of uniformity in its skin structures, e.g. alignment of the guanine platelets in the roll (electronic supplementary material, figure S1) and pitch (figure 3*c*) orientations, a bulk optical axis is formed. This system preserves the polarization aligned with or perpendicular to this axis. These two orientations, as indicated from our measurements, correspond closely to the dorsal–ventral and anterior–posterior axes of the fish.

4.4. Depolarization properties

The other strategic component for polaro-crypsis in the near-surface open ocean environment involves depolarization when the incident polarization angle deviates from the principal axes [4]. Measurements from intact skin of the lookdown exhibited significant depolarization for incoming angles that are not aligned with the principal axes ([4]; see figure 7*a2*–*a6*). This can also be explained from equation (4.1). Depolarization (randomization of the phase of polarized light resulting in a null degree of polarization) in the fish's skin can result from three factors: phase distribution, path length, and the birefringence value ($n_b - n_a$). In the low coherent light reflectors such as the Type 4 guanine platelets, a light ray interacts with a random number of guanine platelets with random yaw orientations, rendering $L(x, y)$ a random variable. Measurements from other marine species indicate that the birefringence value (maximum of $n_b - n_a$) varies from 0.05 to 0.35 [20]. A simple calculation indicates that the minimum path length, $L(x, y)$, should range at least from 1.5 to 10 µm (at $\lambda = 530$ nm) to produce all randomized phases from 0° to 360°. This is well within the measured thickness of the lookdown's iridophore layer (see electronic supplementary material, figure S1h and table S1).

The effect of the guanine platelet system on the polarization state can be evaluated by Mueller matrix operations [32]. In this calculation, each light ray passes through a random number of platelets, bounded by a specified maximum number, and each platelet has a random birefringence ($n_b - n_a$) ranging from 0.05 to 0.35, aligned optical axes and a thickness of 0.1 µm. One hundred thousand ray-paths are averaged together at $\lambda = 530$ nm, and all other scattering and coherent effects are ignored. For incoming horizontally polarized light, the degree of polarization does not change for any number of interacting guanine platelets. For incoming 100% polarized light 45° off the axis, the degree of polarization (both linear and elliptical) reduces to 80, 39 and 3.3% for the specified maximum number of platelets of 10, 20 and 30, respectively. Thus, for non-zero $n_b - n_a$ quantities, the phase becomes random in the x and y plane (the surface of the fish) and the reflected light is efficiently depolarized.

4.5. Collagen birefringence properties

The collagen layer on top of the iridophore layer is highly birefringent (figure 6*c1–c6*) and should have significant influence on the polarization reflection of the fish. The optical axis of the collagen is closely aligned with those of the guanine platelets in the lookdown. So it is likely that the collagen enhances the preservation of incident polarization (when $n_b - n_a = 0$) as well as the depolarization properties by adding an even greater $n_b - n_a$ maximum difference described for the guanine platelets. Because the collagen layer is attached to the skin in a braided mosaic [33], it could be involved with interesting optical effects due to the stress and strain that the fish exerts on its skin when it bends or turns while in motion.

4.6. Angular distribution properties

In addition to the broadband and polarization reflectance, the angular distribution of the reflected light is another important, yet understudied, aspect of animal concealment [2,34]. Many biological materials are heavily pigmented and have a rather simple angular distribution, i.e. a diffuse Lambertian distribution. Biological systems with structural coloration, such as fish, generally have a much more complex angular distribution. Calculating the full angular distribution is difficult because it requires measuring the spectrum and polarization of every possible wavelength and polarization state for every possible incident and reflection angle [35]. Hence usually only an approximation or partial measurement is made for the bidirectional reflectance distribution function (BRDF). The BRDF is an important property to consider for fish when the underwater light fields are not symmetric, e.g. the direct illumination from the sun. A Lambertian diffuse reflectance of sunlight in clear water would make the fish very bright against the background, but having a specular reflection would reflect the sunlight in only one direction, limiting the viewpoints of conspicuousness. Research with beetles has shown that to be camouflaged from all viewing directions, a multilayer reflector would benefit from a transparent scattering layer above the multilayer reflector to convert the narrow angular field of view associated with multilayer reflectors (e.g. iridescence) to a more broad and more diffuse angular field of view [13]. Compared with beetles, fish may have a greater degree of flexibility in how the reflecting platelets can be oriented, thus giving more control over the angular distribution of reflected light.

Quantitative BRDF measurement has been reported for squid (*Pterygioteuthis microlampa*) and hatchet fish (*Sternoptyx* sp.) that inhabit the open ocean [36]. Our qualitative measurements showed that the lookdown's BRDF has a high diffuse component in the anterior–posterior direction and a fairly specular component in the dorsal–ventral direction (electronic supplementary material, figure S6) caused by the random yaw orientation of Type 4 guanine platelets and diffraction due to the narrow width of these platelets. This will have a significant effect on the appearance of the fish in the open ocean. The advantage of this particular optical property for the fish may be related to counter-illumination processes in the vertical direction and intensity averaging processes in the horizontal plane. Counter-illumination is a concealment strategy that involves maintaining the vertical gradient of intensity flux [2]. Hence, as the lookdown is viewed from below or above by a potential predator, adopting a high specular reflectance in this plane will allow the lookdown to mimic the natural radiance distribution in this environment. This particular specular reflectance is likely a product of the lookdown's Type 3 and 4 guanine platelets that have their long axes approximately perpendicular to the water surface. To avoid detection by predators at the same depth as the lookdown, intensity averaging is likely to minimize contrast differences between surface of the skin and background light. BRDF measurements in this plane (parallel to the water surface) indicate that light is scattered diffusely from the lookdown's surface because the tightly packed thin guanine platelets have a random yaw angular distribution and the small dimension in this direction resulting in diffraction. Given the much greater dimension of the long axes of the guanine platelets, they function more like multilayer reflecting mirrors along this direction. It is possible that in the periodically changing light fields in the open ocean, combining diffuse and specular reflectance in a directionally sensitive manner can achieve the best matching to the background.

5. Conclusion

Characterization of the three-dimensional organization of the light reflectors in the skin of the lookdown has revealed a system that is capable of broadband reflectance and polarization reflectance that varies with fish orientation. We have identified four types of guanine platelets distributed in two adjacent layers of the lookdown's skin. The outer layer of iridophores contains large guanine platelets that appear to function as narrow-band multilayer reflectors. The inner layer consists of small guanine platelets that primarily function as a broadband diffuser. The guanine platelets in the lookdown's skin are arranged to enable broadband reflectance, orientation-dependent polarization reflectance and orientation-dependent angular reflectance distribution. Computer simulation based on the physical measurements of guanine platelets confirms the broadband reflectance. The guanine platelets in combination with the collagen layer exhibit bulk optical axes aligned with the principal axes of the fish. This arrangement preserves reflectance polarization when it is parallel or perpendicular to these axes and depolarizes the light when it deviates from these axes with a maximal depolarization at 45° to these axes. Our qualitative BRDF assessment is consistent with the random yaw angle distribution of Type 4 guanine platelets and the orientation of their long axes and demonstrates orientation-specific reflectance distribution. These reflectance properties may facilitate camouflage by fish in the open ocean with changing lighting conditions. Although many marine species have been shown to possess polarization sensitivity, behavioural evidence for polarization crypsis as a strategy for predator evasion by teleost fish remains to be investigated.

Acknowledgements. We thank Julia Cosgrove and Shannon McLellan for excellent technical assistance and Kort Travis for theoretical discussions concerning the paper. We also thank the Texas A&M Supercomputing Facility for providing computing resources for conducting the simulation reported in this paper. The SEM work was carried out at the Core Facilities of Institute of Cellular and Molecular Biology at UT Austin.

Funding statement. This work was supported by a Multidisciplinary University Research Initiative (MURI) grant (N00014-09-1-1054) from the Office of Naval Research of the United States and a grant from NSF (OCE 1130793) to M.E.C. and G.W.K.

References

1. Denton EJ. 1970 On the organization of reflecting surfaces in some marine animals. *Phil. Trans. R. Soc. Lond. B* **258**, 285–313. (doi:10.1098/rstb.1970.0037)
2. Johnsen S. 2003 Lifting the cloak of invisibility: the effects of changing optical conditions on pelagic crypsis. *Integr. Comp. Biol.* **43**, 580–590. (doi:10.1093/icb/43.4.580)
3. Leclercq E, Taylor JF, Migaud H. 2010 Morphological skin colour changes in teleosts. *Fish Fish.* **11**, 159–193. (doi:10.1111/j.1467-2979.2009.00346.x)
4. Brady PC, Travis KA, Maginnis T, Cummings ME. 2013 Polaro-cryptic mirror of the lookdown as a biological model for open ocean camouflage. *Proc. Natl Acad. Sci. USA* **110**, 9764–9769. (doi:10.1073/pnas.1222125110)
5. Johnsen S. 2002 Cryptic and conspicuous coloration in the pelagic environment. *Proc. R. Soc. Lond. B* **269**, 243–256. (doi:10.1098/rspb.2001.1855)
6. Johnsen S, Sosik HM. 2003 Cryptic coloration and mirrored sides as camouflage strategies in near-surface pelagic habitats: implications for foraging and predator avoidance. *Limnol. Oceanogr.* **48**, 1277–1288. (doi:10.4319/lo.2003.48.3.1277)
7. Smith RC. 1974 Structure of solar radiation in the upper layers of the sea. In *Optical aspects of oceanography* (eds NG Jerlov, E Steemann Nielsen), pp. 95–119. London, UK: Academic Press.
8. Partridge JC. 1990 The colour sensitivity and vision of fishes. In *Light and life in the sea* (eds PJ Herring, AK Campbell, M Whitfield, L Maddock), pp. 167–184. Cambridge, UK: Cambridge University Press.
9. Denton EJ, Nicol JAC. 1965 Studies on reflexion of light from silvery surfaces of fishes, with special reference to the bleak, *Alburnus alburnus*. *J. Mar. Biol. Assoc. UK* **45**, 683–703. (doi:10.1017/S0025315400016520)
10. Denton EJ, Land MF. 1971 Mechanism of reflexion in silvery layers of fish and cephalopods. *Proc. R. Soc. Lond. B* **178**, 43–61. (doi:10.1098/rspb.1971.0051)
11. Lythgoe JN, Shand J. 1982 Changes in spectral reflexions from the iridophores of the neon tetra. *J. Physiol.* **325**, 23–34. (doi:10.1113/jphysiol.1982.sp014132)
12. Kasukawa H, Oshima N, Fuji R. 1986 Control of chromatophore movements in dermal chromatic units of blue damselfish. II. The motile iridophore. *Comp. Biochem. Physiol.* **83C**, 1–7.
13. Parker A, Mckenzie D, Large M. 1998 Multilayer reflectors in animals using green and gold beetles as contrasting examples. *J. Exp. Biol.* **201**, 1307–1313.
14. Ouellette F, Krug PA, Stephens T, Dhosi G, Eggleton B. 1995 Broadband and WDM dispersion compensation using chirped sampled fibre Bragg gratings. *Electron. Lett.* **31**, 899–901. (doi:10.1049/el:19950586)
15. McKenzie DR, Yin Y, McFall WD. 1995 Silvery fish skin as an example of a chaotic reflector. *Proc. R. Soc. Lond. A* **451**, 579–584. (doi:10.1098/rspa.1995.0144)
16. Neville AC. 1977 Metallic gold and silver colours in some insect cuticles. *J. Insect Physiol.* **23**, 1267–1274. (doi:10.1016/0022-1910(77)90069-5)
17. Denton EJ, Nicol JAC. 1965 Reflexion of light by external surfaces of the herring, *Clupea Harengus*. *J. Mar. Biol. Assoc. UK.* **45**, 711–738. (doi:10.1017/S0025315400016544)
18. Seago AE, Brady P, Vigneron JP, Schultz TD. 2009 Gold bugs and beyond: a review of iridescence and structural colour mechanisms in beetles (Coleoptera). *J. R. Soc. Interface* **6**, S165–S184. (doi:10.1098/rsif.2008.0354.focus)
19. Vukusic P, Kelly R, Hooper I. 2009 A biological sub-micron thickness optical broadband reflector characterized using both light and microwaves. *J. R. Soc. Interface* **6**, S193–S201. (doi:10.1098/rsif.2008.0345.focus)
20. Jordan TM, Partridge JC, Roberts NW. 2012 Non-polarizing broadband multilayer reflectors in fish. *Nat. Photonics* **6**, 759–763. (doi:10.1038/nphoton.2012.260)
21. Waterman TH. 2006 Reviving a neglected celestial underwater polarization compass for aquatic animals. *Biol. Rev.* **81**, 111–115. (doi:10.1017/S1464793105006883)
22. Cronin TW, Shashar N. 2001 The linearly polarized light field in clear, tropical marine waters: spatial and temporal variation of light intensity, degree of polarization, and e-vector angle. *J. Exp. Biol.* **204**, 2461–2467.
23. You Y *et al*. 2011 Measurements and simulations of polarization states of underwater light in clear oceanic waters. *Appl. Opt.* **50**, 4873–4893. (doi:10.1364/AO.50.004873)
24. Gao M, You Y, Yang P, Kattawar GW. 2012 Backscattering properties of small layered plates: a model for iridosomes. *Opt. Express* **20**, 25 111–25 120. (doi:10.1364/OE.20.025111)
25. Gao M, Yang P, Kattawar GW. 2013 Polarized extinction properties for plates with large aspect ratios. *J. Quant. Spectrosc. Radiat. Transf.* **131**, 72–81. (doi:10.1016/j.jqsrt.2013.03.010)
26. Taflove A, Hagness SC. 2000 *Computational electrodynamics: the finite-difference time-domain method*. Norwood, MA: Artech.
27. Oskooi AF, Roundy D, Ibanescu M, Bermel P, Joannopoulos JD, Steven G, Johnson SG. 2010 MEEP: a flexible free-software package for electromagnetic simulations by the FDTD method. *Comput. Phys. Commun.* **181**, 687–702. (doi:10.1016/j.cpc.2009.11.008)
28. Mäthger LM *et al*. 2013 Bright white scattering from protein spheres in color changing, flexible cuttlefish skin. *Adv. Funct. Mater.* **23**, 3980–3989. (doi:10.1002/adfm.201203705)
29. Harris JE, Hunt S. 1973 The fine structure of iridophores in the skin of Atlantic salmon (*Salmo salar* L.). *Tissue Cell* **5**, 488–497. (doi:10.1016/S0040-8166(73)80039-4)
30. Takeuchi IK. 1976 Electron microscopy of two types of reflecting chromatophores (iridsophores and leucohores) in guppy, *Lebistes reciculatus* Peters. *Cell Tiss. Res.* **173**, 17–27. (doi:10.1007/BF00219263)
31. Bell GRR, Mäthger LM, Gao M, Senft SL, Kuzirian AM, Kattawar GW, Hanlon RT. 2014 Diffuse white structural coloration from multilayer reflectors in a squid. *Adv. Mater.* **26**, 4352–4356. (doi:10.1002/adma.201400383)
32. Goldstein DH. 2011 *Polarized light*, 3rd edn. Boca Raton, FL: CRC Press.
33. Le Guellec D, Morvan-Dubois G, Sire JY. 2004 Skin development in bony fish with particular emphasis on collagen deposition in the dermis of the zebrafish (*Danio rerio*). *Int. J. Dev. Biol.* **48**, 217–232. (doi:10.1387/ijdb.15272388)
34. Vukusic P. 2011 Structural colour: elusive iridescence strategies brought to light. *Curr. Biol.* **21**, R187–R189. (doi:10.1016/j.cub.2011.01.049)
35. Vukusic P, Stavenga DG. 2009 Physical methods for investigating structural colours in biological systems. *J. R. Soc. Interface* **6**, S133–S148. (doi:10.1098/rsif.2008.0386.focus)
36. Haag JM, Jaffe JS, Sweeney AM. 2013 Measurement system for marine animal reflectance functions. *Opt. Express* **21**, 3603–3616. (doi:10.1364/OE.21.003603)